

CHEMISTRY

A European Journal



Accepted Article

Title: Molecular engineering of isomeric benzofurocarbazole donor for photophysical management of thermally activated delayed fluorescent emitters

Authors: Mina Jung, Kyung Hyung Lee, and Jun Yeob Lee

This manuscript has been accepted after peer review and appears as an Accepted Article online prior to editing, proofing, and formal publication of the final Version of Record (VoR). This work is currently citable by using the Digital Object Identifier (DOI) given below. The VoR will be published online in Early View as soon as possible and may be different to this Accepted Article as a result of editing. Readers should obtain the VoR from the journal website shown below when it is published to ensure accuracy of information. The authors are responsible for the content of this Accepted Article.

To be cited as: *Chem. Eur. J.* 10.1002/chem.201905473

Link to VoR: <http://dx.doi.org/10.1002/chem.201905473>

Supported by
ACES

WILEY-VCH

Molecular engineering of isomeric benzofurocarbazole donor for photophysical management of thermally activated delayed fluorescent emitters

Mina Jung, Kyung Hyung Lee, Jun Yeob Lee*

School of Chemical Engineering, Sungkyunkwan University
2066, Seobu-ro, Jangan-gu, Suwon, Gyeonggi, 16419, Republic of Korea

E-mail: leej17@skku.edu

Abstract

The benzofurocarbazole moieties are well-known donor moiety for the design of the thermally activated delayed fluorescence (TADF) emitters. However, only 5*H*-benzofuro[3,2-*c*]carbazole (34BFCz) was reported and no other benzofurocarbazole derivatives were covered in the literature. Herein, two benzofurocarbazole moieties, 12*H*-benzofuro[3,2-*a*]carbazole (12BFCz) and 7*H*-benzofuro[2,3-*b*]carbazole (23BFCz) were synthesized to investigate the effect of donor structure on photophysics and device parameters of TADF emitters. Two benzofurocarbazole derived TADF emitters, 12-(2-(4,6-diphenyl-1,3,5-triazin-2-yl)phenyl)-12*H*-benzofuro[3,2-*a*]carbazole (o12BFCzTrz) and 7-(2-(4,6-diphenyl-1,3,5-triazin-2-yl)phenyl)-7*H*-benzofuro[2,3-*b*]carbazole (o23BFCzTrz), were compared with 5-(2-(4,6-diphenyl-1,3,5-triazin-2-yl)phenyl)-5*H*-benzofuro[3,2-*c*]carbazole (oBFCzTrz). The benzofurocarbazole donor structure governed the TADF characteristics such as charge transfer property and emission color. The 12BFCz donor was effective to blue-shift the emission color and 34BFCz was useful to improve the EQE. The 12BFCz derived o12BFCzTrz showed blue-shifted color coordinate of (0.159, 0.288) compared to (0.178, 0.388) of o23BFCzTrz and (0.169, 0.341) of oBFCzTrz. The 34BFCz derived oBFCzTrz exhibited EQE of 22.9% compared to 19.2% of o12BFCzTrz and 21.1% of o23BFCzTrz.

Keywords: organic light emitting diodes, thermally activated delayed fluorescence, benzofurocarbazole, donor

Accepted Manuscript

Introduction

Organic light-emitting diodes (OLEDs) have been widely researched since the first practical organic electroluminescence device developed by Tang and Van Slyke in 1987.¹ One of the major researches is the development of emitters represented by fluorescent²⁻⁴ and phosphorescent emitters.⁵⁻⁷ Recently, the thermally activated delayed fluorescence (TADF) emitters were developed as the third-generation emitting materials overcoming the drawbacks of fluorescent and phosphorescent emitting materials.⁸⁻¹² The TADF emitters can harvest triplet excitons through efficient up-conversion process by reverse intersystem crossing (RISC) from triplet excited state (T_1) to the singlet excited state (S_1).¹³⁻¹⁴ The TADF material should have a sufficiently small energy gap between S_1 and T_1 (ΔE_{S-T}) for the RISC process by introducing the highest occupied molecular orbital (HOMO)-lowest unoccupied molecular orbital (LUMO) separation.¹⁵⁻¹⁷

In the TADF emitters, electron donor and acceptor moieties are introduced and one of the most common donor moieties is carbazole.¹⁸⁻²² Many carbazole derivatives have been studied because of good electron donor character, easy chemical modification, and thermal stability.²³⁻²⁶ TADF device performances using carbazole derived electron donor moiety are shown in Table S1. Among the many carbazole derived donors, the benzofurocarbazole moiety has been effective as the donors of the TADF materials by tempered the donor character of the carbazole donor.²⁷⁻³⁰ The benzofurocarbazole donor was known as a stable donor moiety enabling high efficiency and stable driving of the TADF emitters. However, only one benzofurocarbazole donor, 5*H*-benzofuro[3,2-*c*]carbazole (34BFCz), was reported in the literature³¹⁻³³ although several benzofurocarbazole isomers are available for TADF emitters. Therefore, the synthesis of benzofurocarbazole isomers and further study about the application of them as the donors of the TADF emitters is needed for enhanced TADF devices performances.

In this work, three isomeric benzofurocarbazole donors were synthesized to study the effect of the donor design on the photophysical and device parameters of the TADF emitters. Three benzofurocarbazole type donors, 12*H*-benzofuro[3,2-*a*]carbazole (12BFCz), 7*H*-benzofuro[2,3-*b*]carbazole (23BFCz), 5*H*-benzofuro[3,2-*c*]carbazole (34BFCz), were used to study the effect of donor structure on the TADF properties of the donor-acceptor type TADF emitters. Two TADF emitters, 12-(2-(4,6-diphenyl-1,3,5-triazin-2-yl)phenyl)-12*H*-benzofuro[3,2*a*]carbazole (o12BFCzTrz), 7-(2-(4,6-diphenyl-1,3,5-triazin-2-yl)phenyl)-7*H*-benzofuro[2,3-*b*]carbazole (o23BFCzTrz) were newly synthesized and they were compared with 5-(2-(4,6-diphenyl-1,3,5-triazin-2-yl)phenyl)-5*H*-benzofuro[3,2-*c*]carbazole (oBFCzTrz) reported in our previous work.²⁹ It was described that the donor structure control in the benzofurocarbazole donor governs the emission color and TADF characteristics of the TADF emitters. Blue shift of the emission color was observed in the o12BFCzTrz and high external quantum efficiency (EQE) was noticed in the oBFCzTrz.

Results and Discussion

Figure 1 shows the chemical structure of the benzofurocarbazole donors synthesized in this work. To investigate the photophysical and device performances of the benzofurocarbazole donor design of TADF, 12BFCz, 23BFCz, and 34BFCz were synthesized as the donors. The 34BFCz was reported in our previous work,²⁷ the 23BFCz has the carbon-carbon linkage at the same position of 34BFCz but oxygen at 2 position of carbazole, and 12BFCz has the oxygen at the same position of 23BFCz but carbon-carbon linkage at 1 position of carbazole. The comparison of the three donors would reveal the effect of oxygen and carbon-carbon linkage position on the donor character of the three donors.

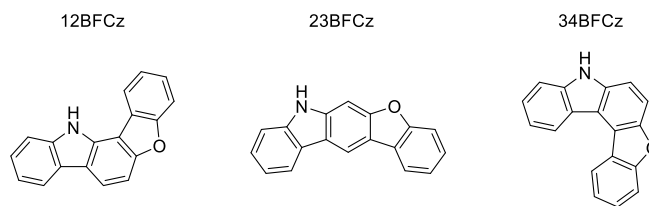
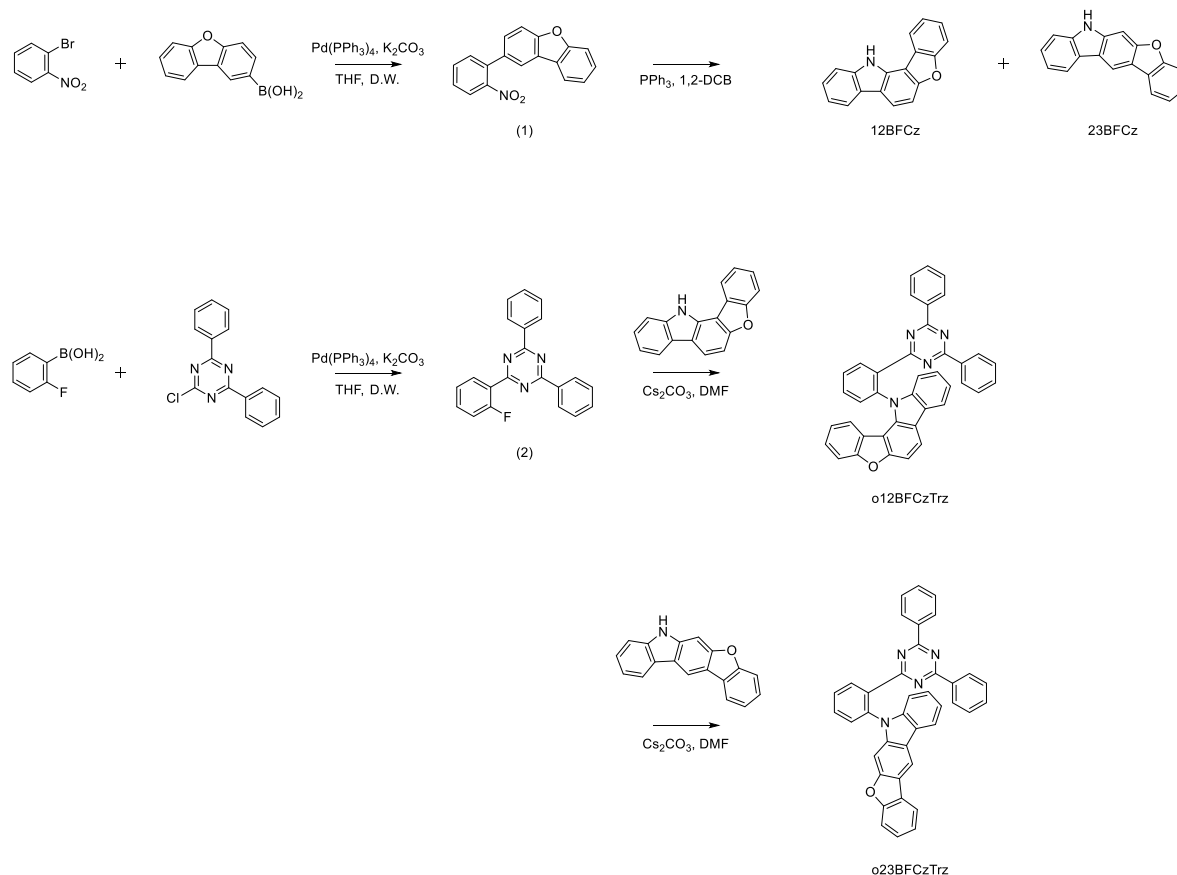


Figure 1. Chemical structure of benzofurocarbazole donor molecules.

The o12BFCzTrz, o23BFCzTrz and oBFCzTrz consisted of a benzofurocarbazole electron donor moiety and a 2,4-diphenyl-1,3,5-triazine electron acceptor moiety interconnected through the ortho- position of a phenyl linker. The ortho- connection concept is well-known in the design of the TADF emitters to strengthen the charge transfer (CT) character and to decrease ΔE_{S-T} by the spatial separation of the HOMO and LUMO orbital distribution.

The synthetic scheme of 12BFCz, 23BFCz, o12BFCzTrz and o23BFCzTrz is shown in Scheme 1. The starting materials, 1-bromo-2-nitrobenzene and dibenzo[*b,d*]furan-2-ylboronic acid were coupled by the Suzuki coupling reaction, and then 12BFCz and 23BFCz were synthesized by ring closing reactions. Then the synthesis of o12BFCzTrz and o23BFCzTrz was carried out using a F functionalized 2,4,6-triphenyl-1,3,5-triazine intermediates and benzofurocarbazole intermediates. The F unit of (2-fluorophenyl)-4,6-diphenyl-1,3,5-triazine was substituted with a synthesized benzofurocarbazole moiety by the Cs_2CO_3 mediated reaction. Synthetic procedures of 34BFCz and oBFCzTrz were described in our previous work.



Scheme 1. Syntheses scheme of o12BFCzTrz and o23BFCzTrz (DW is distilled water).

To estimate the frontier molecular orbitals of 12BFCz, 23BFCz, and 34BFCz, electronic calculation of optimized molecular structure was performed through Gaussian 16 software based on the B3LYP 6-31G* basis set. Figure 2 shows the molecular orbital distribution of benzofurocarbazole donors. The calculated HOMO/LUMO energy levels of 12BFCz, 23BFCz and 34BFCz were -5.43/-0.92, -5.32/-0.92 and -5.30/-0.80 eV, respectively, indicating that the 23BFCz and 34BFCz are stronger donor than 12BFCz. The benzofurocarbazole donors with a linkage through 3 position of carbazole showed shallow HOMO level because the 3 position of carbazole is the HOMO rich position. The benzofuran unit of the benzofurocarbazole affected the HOMO level by the electron sharing through the HOMO dominating 3 position of carbazole.

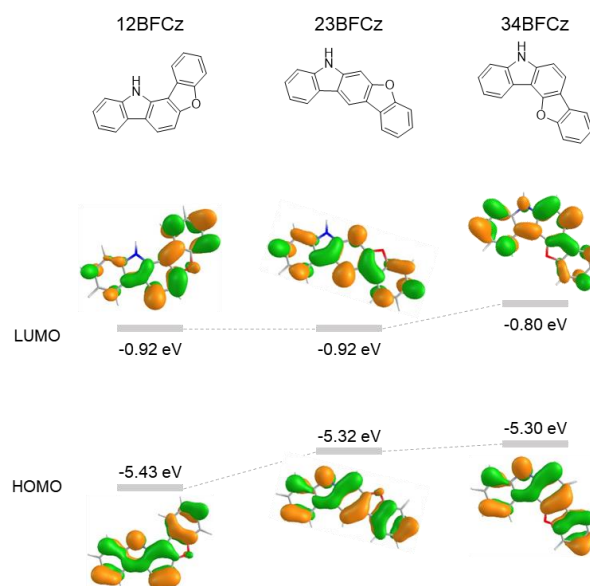


Figure 2. The HOMO-LUMO orbital distribution of the benzofurocarbazole moieties. The DFT calculation results using Gaussian 16 software based on the B3LYP 6-31G* basis set.

Overall material characteristics of o12BFCzTrz, o23BFCzTrz and oBFCzTrz were also estimated by electronic calculation of the optimized molecular structure and orbital distribution. Figure 3 shows the calculated optimized structure and the molecular orbital distribution of o12BFCzTrz, o23BFCzTrz and oBFCzTrz. Gaussian 16 software based on the B3LYP 6-31G* basis set was used for the calculation of the TADF molecules. The donor moiety had little effect on the HOMO and LUMO distribution. In all materials, the HOMO was dispersed over the benzofurocarbazole electron-donating group, and the LUMO was dominantly dispersed in the diphenyltriazine electron acceptor moiety. The $n-\pi^*$ electron interaction between triazine moiety and non-bonding electron of nitrogen in benzofurocarbazole was also similar in all three TADF phenyl linker.³⁴ The dihedral angles between phenyl linker and diphenyltriazine moiety of three compounds were similarly in the range of 35-38°. The calculated LUMO energy level was also similar in the three compounds. On the other hand, the dihedral angles between benzofurocarbazole and phenyl linker of o12BFCzTrz, o23BFCzTrz and oBFCzTrz were 77.7, 66.7, and 68.8°, respectively. In the

case of o12BFCzTrz, the donor was largely distorted due to the steric hindrance between the phenyl molecules. The torsion angle between linker and benzofuran unit of benzofurocarbazole oriented to the phenyl linker direction.

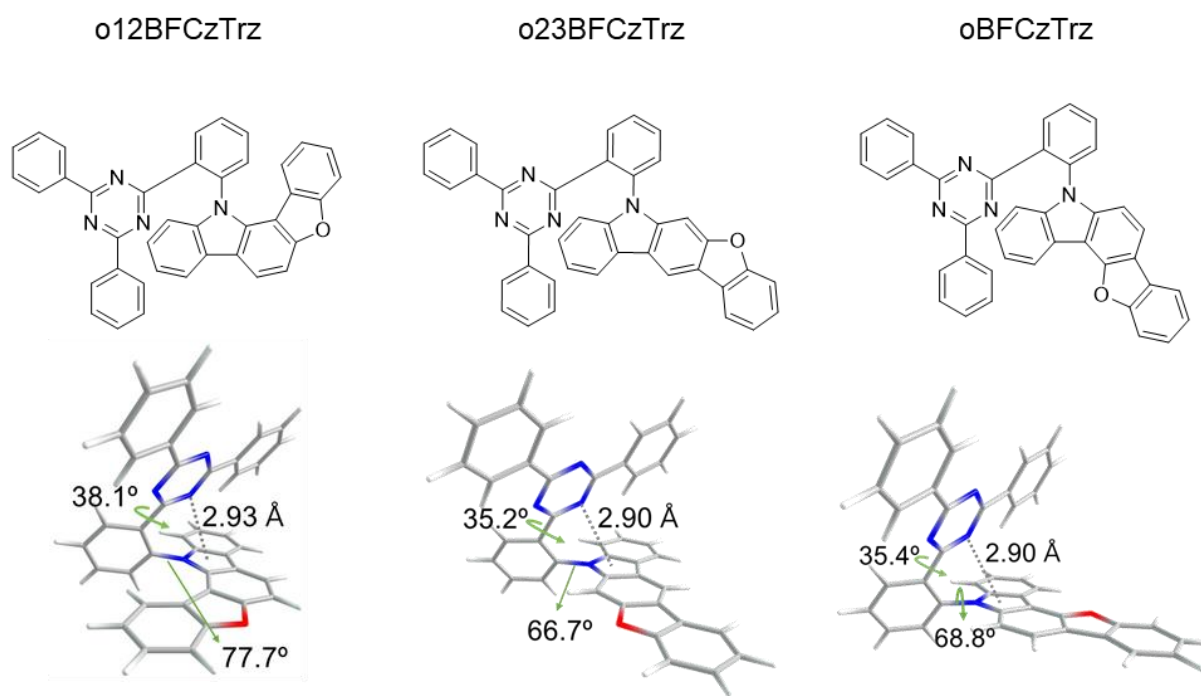


Figure 3. The calculated optimized structures of o12BFCzTrz, o23BFCzTrz and oBFCzTrz.

The calculated HOMO energy levels of o12BFCzTrz, o23BFCzTrz, and oBFCzTrz were -5.27, -5.20, and -5.18 eV, respectively. The HOMO level of the TADF emitters was dominated by the donor moiety because the HOMO was localized on the donor moiety (Figure S1). The shallow HOMO level of the 23BFCz and 34BFCz donors with nitrogen at 3 position of dibenzofuran resulted in the shallow HOMO in the o23BFCzTrz and oBFCzTrz emitters. All calculated data of the TADF emitters are presented in Table 1.

Table 1. The calculated data of the o12BFCzTrz, o23BFCzTrz and oBFCzTrz.

o12BFCzTrz	o23BFCzTrz	oBFCzTrz
------------	------------	----------

LUMO ^[a]	- 1.84 eV	- 1.84 eV	- 1.86 eV
HOMO ^[a]	- 5.27 eV	- 5.20 eV	- 5.18 eV
LUMO ^[b]	- 3.38 eV	- 3.41 eV	- 3.40 eV
HOMO ^[b]	- 6.15 eV	- 6.07 eV	- 6.10 eV

^[a] The calculation based on the B3LYP 6-31G* basis set.

^[b] The measured values by cyclic voltammetry (CV).

The calculated HOMO and LUMO values were confirmed experimentally by cyclic voltammetry (CV). The HOMO/LUMO levels of o12BFCzTrz, o23BFCzTrz and oBFCzTrz were estimated to be -6.15/-3.38, -6.07/-3.41 and -6.10/-3.40 eV, respectively (Figure S2).

The trend of the HOMO/LUMO levels coincided with the calculation results.

The photophysical analysis of the TADF emitters was performed to correlate the donor structure with the light absorption and emission behaviors. Figure S3 shows the ultraviolet-visible (UV-Vis) absorption spectra of the TADF emitters. The UV/Vis absorption data provided strong absorption bands below $\lambda = 355$ nm assigned to $n-\pi^*$ transition and $\pi-\pi^*$ transition of the donor-acceptor skeletons, and broad absorption bands between 360 and 440 nm assigned to intramolecular CT absorption. The CT absorption of the o23BFCzTrz and oBFCzTrz emitters was rather strong because of the strong donor strength of the 23BFCz and 34BFCz donors embedded in the two TADF materials, respectively. The UV-Vis absorption edges of the o12BFCzTrz, o23BFCzTrz and oBFCzTrz emitters were 431, 443, and 448 nm, respectively. The absorption edge of o12BFCzTrz was relatively positioned at short wavelength by the weak CT character attributed to the weak 12BFCz donor.

Differences in the CT characteristics can also be seen in the PL spectra measured in solvents with different polarities. (Figure S4). In the PL measurement of the emitters in toluene and methylene chloride, the PL peak position was red-shifted by 40 nm in the o23BFCzTrz (476 to 516 nm) and oBFCzTRZ (477 to 518 nm), while it was bathochromically shifted only by

22.5 nm in the o12BFCzTrz (495.5 to 473 nm). This supports the weak CT character of the o12BFCzTrz emitter.

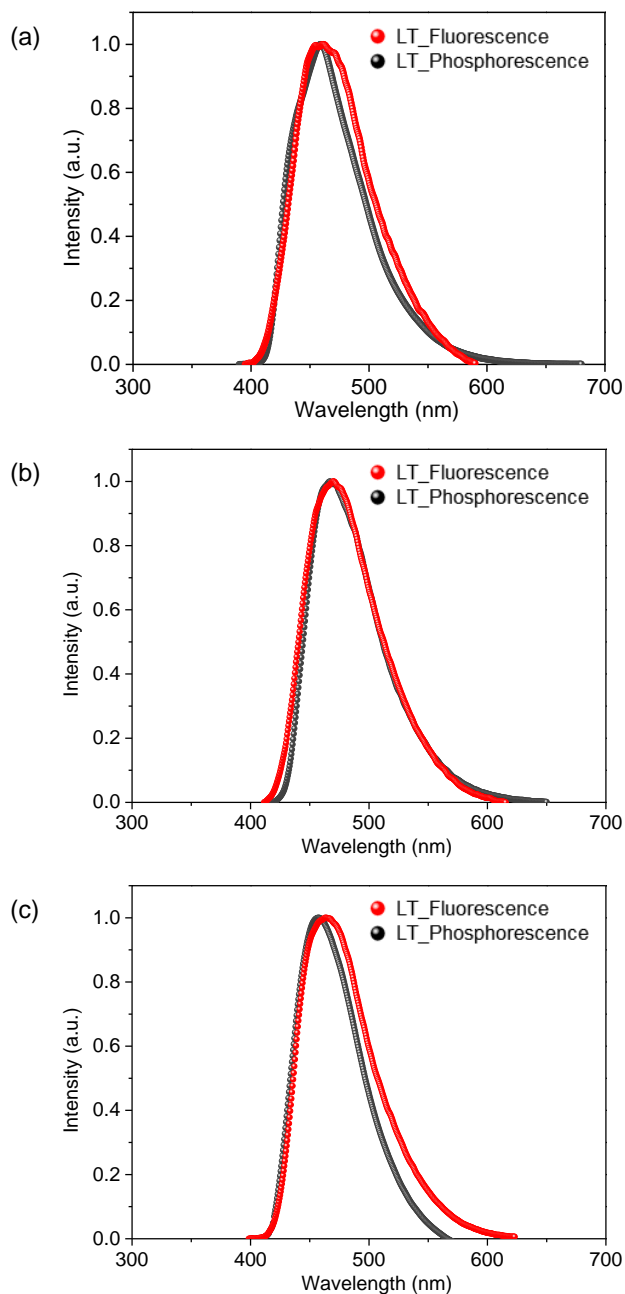


Figure 4. The fluorescence and phosphorescence spectra of o12BFCzTrz (a), o23BFCzTrz (b) and oBFCzTrz (c) at 77 K.

Table 2. Photophysical data of the o12BFCzTrz, o23BFCzTrz and oBFCzTrz.

	o12BFCzTrz	o23BFCzTrz	oBFCzTrz
Band gap ^[a]	2.77 eV	2.66 eV	2.70 eV
Singlet energy ^[b]	3.092 eV	3.000 eV	2.994 eV
Triplet energy ^[c]	3.077 eV	2.958 eV	2.992 eV
ΔE_{S-T}	0.015 eV	0.042 eV	0.002 eV

^[a]Measured by the cyclic voltammetry. ^[b]Singlet energy was calculated from the onset wavelength of fluorescence emission. ^[c]Triplet energy was calculated from the onset wavelength of phosphorescence emission.

The photoluminescence (PL) emission spectra of the o12BFCzTrz, o23BFCzTrz and oBFCzTrz emitters collected from THF solution (1.0×10^{-5} M) at low temperature (77 K) are in Figure 4. ΔE_{S-T} of TADF molecules were estimated from the low-temperature fluorescence and phosphorescence data.³⁵ The measured singlet/triplet energy of o12BFCzTrz, o23BFCzTrz and oBFCzTrz were 3.09/3.08, 3.00/2.96, and 2.99/2.99 eV, respectively (Table 2). In the case of singlet energy, o12BFCzTrz exhibited high singlet energy due to weak CT character relative to o23BFCzTrz and oBFCzTrz as can be estimated from the weak donor character of 12BFCz. The triplet energy was also high in the o12BFCzTrz by the large distortion of the donor from the phenyl linker which hinders the extension of the degree of conjugation. All three TADF molecules showed CT emission characters in the fluorescence spectra. In the case of phosphorescence, the o12BFCzTrz showed combined emission from local and CT triplet excited states by the weak CT character, but the o23BFCzTrz and oBFCzTrz exhibited CT dominant triplet emission by the strong CT character.

Table 3. Photophysical properties of o12BFCzTrz, o23BFCzTrz and oBFCzTrz

PLQY (%)	τ_{prompt} (ns)	τ_{delayed} (μ s)	k_p (10^7 s ⁻¹)	k_d (10^5 s ⁻¹)	Φ_F	Φ_{TADF}	k_r^S (10^7 s ⁻¹) ^[a]	k_{nr}^S (10^7 s ⁻¹) ^[a]	k_{ISC} (10^7 s ⁻¹) ^[a]	k_{RISC} (10^5 s ⁻¹) ^[a]

o12BFCzTrz	82.7	35.2	4.09	2.84	2.44	0.27	0.56	2.08	0.435	0.318	2.76
o23BFCzTrz	85.7	24.8	4.22	4.03	2.37	0.47	0.38	3.12	0.542	0.364	2.61
oBFCzTrz	88.7	32.9	3.06	3.04	3.27	0.50	0.39	2.62	0.548	0.082	3.37

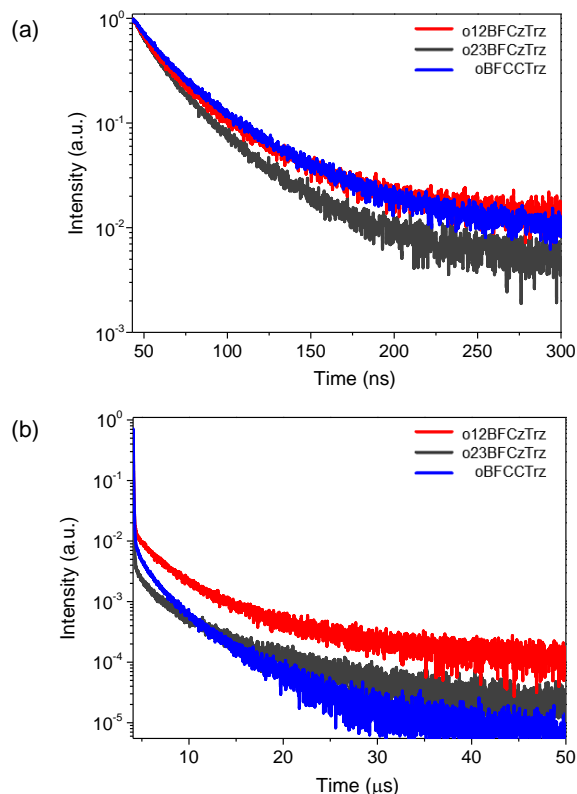


Figure 5. Transient PL results showing prompt component (a) and delayed fluorescence component (b) of o12BFCzTrz, o23BFCzTrz and oBFCzTrz.

Figure 5 represents transient PL decays of o12BFCzTrz, o23BFCzTrz and oBFCzTrz. The lifetime of prompt/delayed component of o12BFCzTrz, o23BFCzTrz and oBFCzTrz was 35.21 ns/4.09 μ s, 24.8 ns/4.22 μ s, and 32.9 ns/3.06 μ s, respectively. The RISC rate constants (k_{RISC}) of o12BFCzTrz, o23BFCzTrz and oBFCzTrz by calculation from the transient PL decay were 2.61, 2.76, and 3.37×10^5 , respectively.³⁶ The oBFCzTrz showed a fast RISC process due to the small $\Delta E_{\text{S-T}}$. The PL quantum yields (PLQYs) of o12BFCzTrz, o23BFCzTrz and oBFCzTrz measured under a nitrogen condition were 82.7, 85.2 and 88.7%, respectively. All material analysis data are summarized in Table 3.

The photophysical study of the o12BFCzTrz, o23BFCzTrz and oBFCzTrz emitters proposed that they would function as TADF emitters. Therefore, OLED devices doped with o12BFCzTrz, o23BFCzTrz and oBFCzTrz in the emitting layer were fabricated using bis[2-(diphenylphosphino)phenyl] ether oxide (DPEPO) host. Device structure is explained in the Experimental section and Figure S5. The concentration of the TADF dopant was optimized to 20 wt%, and data at other concentrations can be found in supporting information (Figure S6, Table S2). The device behavior of the oBFCzTrz, o23BFCzTrz and oBFCzTrz is presented in Figure 6. The current density and luminance to driving voltage curves of the devices are shown in Figure 6 (a). The EQE values of TADF devices are plotted in Figure 6 (b). In the case of maximum EQE, o12BFCzTrz, o23BFCzTrz, and oBFCzTrz showed EQEs of 19.2, 21.1 and 22.9%, respectively. The relative order of the EQE was in agreement with that of the PLQY, suggesting that the PLQY is the critical factor for the EQE. The electroluminescence (EL) spectra in Figure 6 (c) showed that the EL emission is blue-shifted in the o12BFCzTrz as can be projected from the PL spectra. The o23BFCzTrz and oBFCzTrz devices with strong CT properties, showed CIE color coordinates of (0.18, 0.39) and (0.17, 0.34), respectively, whereas that of the o12BFCzTrz was (0.16, 0.29). All device performances are summarized in Table 4.

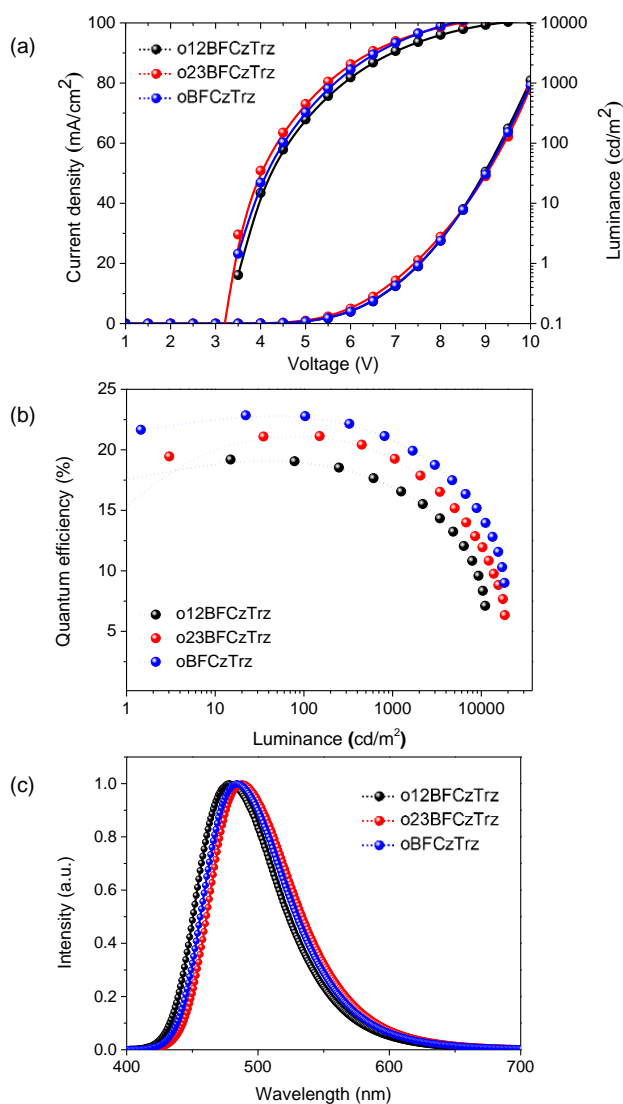


Figure 6. The current density-voltage-luminance (a), EQE-luminance (b) and EL spectra (c) of o12BFCzTrz, o23BFCzTrz, and oBFCzTrz devices.

Table 4. The device performances of o12BFCzTrz, o23BFCzTrz and oBFCzTrz.

	o12BFCzTrz	o23BFCzTrz	oBFCzTrz
EQE _{max} (%)	19.2	21.1	22.9
Power efficiency _{max} (lm W ⁻¹)	30.3	41.2	42.4
Current efficiency _{max} (cd A ⁻¹)	37.2	49.6	49.5
CIE (x, y)	(0.159, 0.288)	(0.178, 0.388)	(0.169, 0.341)
EL _{max} (nm)	478	484	488

Conclusion

In conclusion, the synthesis of benzofurocarbazole electron donor moieties, 12BFCz, 23BFCz, and 34BFCz, and application of them as the donors of the TADF emitters revealed that the 12BFCz donor was effective to blue-shift the emission color and 34BFCz was useful to improve the EQE. The 12BFCz derived 12BFCzTrz showed blue-shifted color coordinate of (0.159, 0.288) compared to (0.178, 0.388) of o23BFCzTrz and (0.169, 0.341) of oBFCzTrz. The 34BFCz derived oBFCzTrz exhibited EQE of 22.9% compared to 19.2% of o12BFCzTrz and 21.1% of o23BFCzTrz. Therefore, the molecular management of the benzofurocarbazole donor could selectively control the device performances of the TADF OLEDs.

Corresponding author

Correspondence to Prof. Jun Yeob Lee (leej17@skku.edu)

References

- [1] C. W. Tang, S. A. VanSlyke, *Appl. Phys. Lett.* 1987, 51, 913.
- [2] J. Shia, C. W. Tang, *Appl. Phys. Lett.* 2002, 80, 3201.
- [3] Y. Sun, L. Duan, D. Zhang, J. Qiao, G. Dong, L. Wang, Y. Qiu, *Adv. Funct. Mater.* 2011, 21, 1881–1886.
- [4] M. Jung, J. Lee, H. Jung, S. Kang, A. Wakamiya, J. Park, *Dyes. Pigm.* 2018, 158, 42-49.
- [5] M. A. Baldo, D. F. O'Brien, Y. You, A. Shoustikov, S. Sibley, M. E. Thompson, S. R. Forrest, *Nature* 1998, 395, 151–154.
- [6] C. Adachi, M. A. Baldo, M. E. Thompson, S. R. Forrest, *J. Appl. Phys.* 2001, 90, 10.
- [7] Y. Seino, H. Sasabe, Y. –J. Pu, J. Kido, *Adv. Mater.* 2014, 26, 1612–1616.

- [8] K. Sato, K. Yoshimura, T. Kai, A. Kawada, H. Miyazaki, C. Adachi, *Appl. Phys. Lett.* 2011, 98, 083302.
- [9] J. Lee, K. Shizu, H. Tanaka, H. Nomura, T. Yasuda, C. Adachi, *J. Mater. Chem. C* 2013, 1, 4599–4604.
- [10] Y. J. Cho, S. K. Jeon, B. D. Chin, E. Yu, J. Y. Lee, *Angew. Chem. Int. Ed.* 2015, 54, 5201–5204.
- [11] Y. Liu, G. Xie, K. Wu, Z. Luo, T. Zhou, X. Zeng, J. Yu, S. Gong, C. Yang, *J. Mater. Chem. C* 2016, 4, 4402–4407.
- [12] M. Jung, K. H. Lee, W. P. Hong, J. Y. Lee, *J. Mater. Chem. C* 2019, 7, 7760–7767.
- [13] A. Jablonski, *Nature* 1933, 131, 839–840.
- [14] G. N. Lewis, D. Lipkin, T. T. Magel, *J. Am. Chem. Soc.* 1941, 63, 3005–3018.
- [15] H. Kaji, H. Suzuki, T. Fukushima, K. Shizu, K. Suzuki, S. Kubo, T. Komino, H. Oiwa, F. Suzuki, A. Wakamiya, Y. Murata, C. Adachi, *Nature Commun.* 2015, 6, 8476.
- [16] J. Lee, K. Shizu, H. Tanaka, H. Nakanotani, T. Yasuda, H. Kaji, C. Adachi, *J. Mater. Chem. C* 2015, 3, 2175–2181.
- [17] L. -S. Cui, H. Nomura, Y. Geng, J. U. Kim, H. Nakanotani, C. Adachi, *Angew. Chem. Int. Ed.* 2017, 56, 1571–1575.
- [18] T. Serevicius, T. Nakagawa, M. -C. Kuo, S. -H. Cheng, K. -T. Wong, C. -H. Chang, R. C. Kwong, S. Xiae, C. Adachi, *Phys. Chem. Chem. Phys.* 2013, 15, 15850–15855.
- [19] D. Zhang, X. Cao, Q. Wu, M. Zhang, N. Sun, X. Zhang, Y. Tao, *J. Mater. Chem. C* 2018, 6, 3675–3682.
- [20] M. Kim, S. K. Jeon, S. -H. Hwang, S. Lee, E. Yu, J. Y. Lee, *Chem. Commun.* 2016, 52, 339–342.
- [21] Y. Im, S. H. Han, J. Y. Lee, *J. Mater. Chem. C* 2018, 6, 5012–5017.
- [22] H. Uoyama, K. Goushi, K. Shizu, H. Nomura, C. Adachi, *Nature* 2012, 492, 234–238.
- [23] J. -R. Cha, C. W. Lee, J. Y. Lee, M. -S. Gong, *Dyes. Pigm.* 2016, 134, 562–568

- [24] D. Karthik, S. Y. Lee, D. H. Ahn, H. Lee, J. Y. Lee, J. H. Kwon, J. H. Park, *Org. Electron.* 2019, 74, 282–289.
- [25] P. Rajamalli, N. Senthilkumar, P. Gandeepan, C. –C. R. -Wu, H. –W. Lin, C –H. Cheng, *ACS Appl. Mater. Interfaces* 2016, 8, 27026–27034.
- [26] Q. Zhang, S. Sun, W. J. Chung, S. J. Yoon, Y. Wang, R. Guo, S. Ye, J. Y. Lee, L. Wang, *J. Mater. Chem. C* 2019, 7, 12248-12255.
- [27] D. R. Lee, S. –H. Hwang, S. K. Jeon, C. W. Lee, J. Y. Lee, *Chem. Commun.* 2015, 51, 8105-8107.
- [28] C. Bian, Q. Wang, Q. Ran, X. –Y. Liu, J. Fan, L. -S. Liao, *Org. Electron.* 2018, 52, 138–145.
- [29] D. R. Lee, J. M. Choi, C. W. Lee, J. Y. Lee, *ACS Appl. Mater. Interfaces* 2016, 8, 23190–23196.
- [30] Q. Zhang, S. Xiang, Z. Huang, S. Sun, S. Ye, X. Lv, W. Liu, R. Guo, L. Wang, *Dyes. Pigm.* 2018, 155, 51–58.
- [31] M. –S. Gong, J. –R. Cha, C. W. Lee, *Org. Electron.* 2017, 42, 66-74.
- [32] C. Bian, Q. Wang, X. –Y. Liu, J. Fan, L. –S. Liao, *Org. Electron.* 2017, 46, 105-114.
- [33] H. L. Lee, K. H. Lee, J. Y. Lee, W. P. Hong, *J. Mater. Chem. C* 2019, 7, 6465—6474.
- [34] X.-K. Chen, B. W. Bakr, M. Auffray, Y. Tsuchiya, C. D. Sherrill, C. Adachi, J. –L. Bredas, *J. Phys. Chem. Lett.* 2019, 10, 3260–3268.
- [35] R. S. Nobuyasu, Z. Ren, G. C. Griffiths, A. S. Batsanov, P. Data, S. Yan, A. P. Monkman, M. R. Bryce, F. B. Dias, *Adv. Optical Mater.* 2016, 4, 597–607.
- [36] H. Noda, H. Nakanotani, C. Adachi, *Sci. Adv.* 2018, 4, eaao6910.

Accepted Manuscript